Biogeochemistry
https://doi.org/10.1007/s10533-022-00977-x

Unraveling the role of sulfide-natural organic matter interplay on methane cycling in anoxic environments

Edgardo I. Valenzuela · Casey Bryce · Judith Forberg · Britta Planer-Friedrich · Andreas Kappler · Francisco J. Cervantes

Received: 10 May 2022 / Accepted: 19 September 2022

Abstract Redox-active natural organic matter (NOM) possesses great potential to fuel chemical and biological reactions due to its electron-transferring capacity. Chemical sulfide oxidation with redox-active NOM as the terminal electron acceptor (TEA) has been shown to determine the extent to which organic matter degradation produces CO_2 or CH_4 by suppressing methanogenesis. However, the effect that such S cycling reactions potentially have on CH_4-consuming processes, such as sulfate- and NOM-dependent anaerobic oxidation of methane (AOM), is yet to be disclosed. In this study, bulk Pahokee Peat humic substances (PPHS) were employed as a model source of redox-active NOM to test their role as TEA for the chemical oxidation of dissolved sulfide. While elemental sulfur was the dominant product of sulfide oxidation (~50 to 75% of oxidized sulfur), thiosulfate was the second most abundant product accounting for ~20% of the oxidized sulfide. The incorporation of S into PPHS' organic structure was revealed by the formation of methylthio, ethylthio, thiol, and aromatic-disulfide/polysulfide moieties after the reaction, which may compromise the availability of NOM to act as TEA for the oxidation of organic matter or methane. Wetland sediment incubations amended with sulfate and PPHS revealed that PPHS were the preferential TEA for catalyzing AOM (NOM-AOM) while sulfate suppressed methanogenic activities. Considering this and several novel findings concerning sulfate- and NOM-driven AOM, we discuss novel mechanisms by which sulfur/organic matter interactions could impact the microbial processes of CH_4 production and consumption.

Responsible Editor: Marguerite A. Xenopoulos.

Supplementary Information The online version contains supplementary material available at https://doi.org/10.1007/s10533-022-00977-x.

E. I. Valenzuela (✉)
División de Ciencias Ambientales, Instituto Potosino de Investigación Científica y Tecnológica, Camino a la Presa San José 2055, Lomas 4ta Sección, 78216 San Luis Potosí, Mexico

E. I. Valenzuela · F. J. Cervantes (✉)
Laboratory for Research on Advanced Processes for Water Treatment, Engineering Institute, Campus Juriquilla, Universidad Nacional Autónoma de México (UNAM), Blvd. Juriquilla 2001, 76230 Querétaro, Mexico
e-mail: fcervantesc@iingen.unam.mx

C. Bryce
School of Earth Sciences, University of Bristol, Bristol, UK

J. Forberg · B. Planer-Friedrich
Environmental Geochemistry, Bayreuth Center for Ecology and Environmental Research (BayCEER), University of Bayreuth, 95447 Bayreuth, Germany

A. Kappler
Geomicrobiology, Department of Applied Geosciences, University of Tuebingen, Tuebingen, Germany

Published online: 30 September 2022

Keywords Cryptic sulfur cycling · Anaerobic methanotrophy · Sulfate reduction · Natural organic matter

Introduction

The redox-active fraction of natural organic matter (NOM), traditionally known as humus or humic substances, takes part in several natural transformations by catalyzing redox reactions (Stevenson 1983; MacCarthy 2007). These processes, which can be of chemical or biological nature, are inherently located within several biogeochemical cycles where they play critical roles in regulating the fluxes of key elements (Martinez et al. 2013; Lipczynska-Kochany 2018). The electron-transferring moieties in NOM, largely comprised of quinones (Scott et al. 1998; Hernández-Montoya et al. 2012), can fuel the oxidation of many organic and inorganic compounds by functioning as terminal electron acceptors (TEA) (Lovley et al. 1996; Bai et al. 2019). In organic-rich environments such as wetlands, redox-active NOM influences the biogeochemical processes of organic matter degradation by impacting the emission of greenhouse gases (Keller et al. 2009; Hopple et al. 2019; Rush et al. 2021). For instance, redox-active NOM affects the CO_2:CH_4 emission ratio by means of the suppression of CH_4 production provoked by its function as TEA for the mineralization of labile organic compounds (Cervantes et al. 2002, 2008). The anaerobic oxidation of methane (AOM) is a key microbial process that prevents the emission of vast amounts of this greenhouse gas into the atmosphere (Caldwell et al. 2008; Cui et al. 2015). While most AOM reactions usually proceed with several inorganic compounds as TEA (i.e., sulfate, iron, manganese, nitrate/nitrite, arsenate, etc.) (Raghoebarsing et al. 2006; Knittel and Boetius 2009; Beal et al. 2009; Ettwig et al. 2010; Leu et al. 2020; Shi et al. 2020), recent reports have shown that redox-active NOM can also serve as the TEA for this process in a so-called NOM-driven AOM (NOM-AOM, Eq. 1) (Valenzuela and Cervantes 2021).

$$\mathrm{CH_4 + 4Q \cdot NOM_{ox} + 2H_2O \rightarrow CO_2 + 4QH_2 \cdot NOM_{red}}$$
$$\Delta\, \mathrm{G^{o'}(kJ\ mol^{-1}) = -\ 30\ to\ -\ 417^*} \quad (1)$$

*Further details on this and all thermodynamic calculations involving redox-active natural organic matter (NOM) are described in Table S3. $Q{\cdot}NOM_{ox}$ refers to oxidizing equivalents stored as quinones in oxidized NOM, while $QH_2{\cdot}NOM_{red}$ refers to reducing equivalents stored as hydroquinones in reduced NOM.

This process occurs in several environments including the sediments of coastal tropical wetlands (Valenzuela et al. 2017, 2019), the water column of marginal seas (van Grinsven et al. 2020), methanogenic lake sediments (Vigderovich et al. 2022), and has also been documented under artificial conditions by microbiota of deep-sea seep sediments (Scheller et al. 2016). Nonetheless, chemical and biological reactions simultaneously taking place in the surrounding environment in which NOM-AOM takes place will determine the extent in which this process can contribute to the diminishment of CH_4 emissions. For instance, redox-active NOM possesses a wide range of redox potentials (−0.3 to +0.3 V), which makes it greatly reactive toward many substances in the environment by driving redox reactions of high thermodynamic feasibility (Straub et al. 2000; Aeschbacher et al. 2011; Tian et al. 2018). Considering this, inorganic electron donors, such as dissolved sulfide, sourced from microbial sulfur-reducing processes, can easily be abiotically oxidized by redox-active NOM and produce distinct oxidized sulfur compounds as products (Eqs. 2 to 4) (Yu et al. 2015; Yu et al. 2016a, b).

$$\mathrm{HS^- + Q \cdot NOM_{ox} + H^+ \rightarrow S^0 + QH_2{\cdot}NOM_{red}}$$
$$\mathrm{\Delta G^{o'}(kJ\ mol^{-1}) = +62\ to\ -401} \quad (2)$$

$$\mathrm{2HS^- + 4Q \cdot NOM_{ox} + 3H_2O \rightarrow S_2O_3^{2-} + 4QH_2{\cdot}NOM_{red}}$$
$$\mathrm{\Delta G^{o'}(kJmol^{-1}) = +248\ to -215} \quad (3)$$

$$\mathrm{HS^- + 4Q \cdot NOM_{ox} + 4H_2O \rightarrow SO_4^{2-}}$$
$$\mathrm{+\ 4QH_2{\cdot}NOM_{red} + H^+\ \Delta G^{o'}(kJ\ mol^{-1})} \quad (4)$$
$$\mathrm{= +62\ to\ -401}$$

Such types of reactions often remain cryptic given their rapid and transitory occurrence; yet, this phenomenon is expected to partly drive the ratio of CH_4:CO_2 emitted from ecosystems, which is a key parameter due to the impact of these greenhouse

gases on climate change (Heitmann and Blodau 2006; Heitmann et al. 2007; Yu et al. 2016a). Likewise, the recycling of sulfur prompted by the oxidizing capacity of NOM could indirectly extend the occurrence of AOM processes, which rely on the reduction of oxidized sulfur compounds, such as sulfate (SO_4^{2-}) or thiosulfate ($S_2O_3^{2-}$) (Eqs. 5 and 6) (Cassarini et al. 2017; Bhattarai et al. 2019). In addition, given that the partial pressure of H_2S will be kept relatively low due to its abiotic oxidation, the thermodynamic feasibility of the AOM reactions relying on the reduction of oxidized sulfur compounds will be positively affected.

$$CH_4 + SO_4^{2-} \rightarrow HS^- + HCO_3^- + H_2O \quad \Delta G^{o'}(\text{kJ mol}^{-1}) = -17 \tag{5}$$

$$CH_4 + S_2O_3^{2-} \rightarrow 2HS^- + HCO_3^- + H^+ \quad \Delta G^{o'}(\text{kJ mol}^{-1}) = -39 \tag{6}$$

Besides, given its recent discovery, few environmental factors affecting NOM-AOM have been determined (Valenzuela and Cervantes 2021). In this context, it remains an open question whether competing electron donors, such as reduced sulfur compounds (e.g., sulfide) could hinder NOM-AOM by reacting with the redox-active moieties in NOM, thus decreasing its electron-accepting capacity, which is indispensable for sustaining CH_4 oxidation. For these reasons, it is crucial to evaluate how NOM-driven S-oxidation processes will impact CH_4-consuming and -producing processes, which will likely be determined by: (i) the amount and type of oxidized S intermediaries generated, (ii) the competition between microbes and reduced S species for the reduction of NOM functional moieties, and (iii) the type and metabolism of microorganisms driving the key metabolic processes in ecosystems. In this paper, chemical and biological experiments in which relevant conditions emulating natural anoxic environments in which sulfate- and NOM-reducing processes prevail were implemented to analyze the effect that NOM-driven sulfide oxidation has on CH_4-consuming and -producing reactions. Firstly, with the purpose of anticipating the organic and inorganic sulfur oxidation products originated by reaction with redox-active NOM, abiotic assays were performed employing commercially available humic substances as an analogue of naturally occurring redox-active organic matter. Therefore, a real scenario in which sulfate- and NOM-reducing processes co-occur was emulated by means of biotic tests inoculated with sediments collected from a coastal wetland constantly receiving inputs of sulfate-rich seawater under CH_4-consuming and -producing conditions. Based on novel findings obtained by these approaches, several avenues of research that are essential to unveil the impact that NOM-driven cryptic cycling of S can have on the emission of greenhouse gases from organotrophic environments are identified.

Materials and methods

Medium preparation and experimental setup

Pahokee Peat humic substances (PPHS, obtained from the International Humic Substances Society, catalog number 1S103H) were employed as a redox-active NOM model. This source of NOM was selected due to its characteristics, such as redox potential (~0.794 V) (Struyk and Sposito 2001) and electron accepting capacity (1648 ± 30 µmol e-/g PPHS) (Aeschbacher et al. 2010). PPHS were suspended overnight in an artificial basal medium by magnetic stirring under oxic conditions (open to air) at 200 rpm. This was done with two purposes: (i) obtaining a suspension of the whole content of the humic material, which includes soluble (comparable to dissolved organic matter) and insoluble fractions (comparable to particulate organic matter), and (ii) to achieve the complete oxidation of those redox-active moieties in PPHS that could be in a reduced state in the untreated material. The basal medium employed as a background for the abiotic reaction between sulfide and PPHS was the same used for the subsequent biological incubations. This was done to identify those products of sulfide oxidation in a controlled environment which excluded the sediment employed as the model of study in the biological incubations. This basal medium was selected for its suitability for enriching anaerobic microorganisms and its absence of additional carbon sources which could compete with CH_4 as an electron donor in the methanotrophy experiments. Its composition was as follows (in g L^{-1}), modified from Cervantes et al. 2000):NH_4Cl (0.3), K_2HPO_4 (0.2), $MgCl_2{\cdot}6H_2O$ (0.03), and $CaCl_2$ (0.1). Trace elements were included in the medium by

adding 1 mL L^{-1} of a solution with the following composition (in mg L^{-1}):$FeCl_2{\cdot}4H_2O$ (2000), H_2BO_3 (50), $ZnCl_2$ (50), $CuCl_2{\cdot}6H_2O$ (90), $MnCl_2{\cdot}4H_2O$ (500), $AlCl_3{\cdot}6H_2O$ (90), $CoCl_2{\cdot}6H_2O$ (2000), $NiCl{\cdot}6H_2O$ (920), $Na_2SeO{\cdot}5H_2O$ (162), $(NH_4)_6Mo_7O_{24}$ (500), EDTA (1000), $Na_2WO_4{\cdot}H_2O$ (100), and 1 mL L^{-1} HCl at 36%. Additionally, NaCl (3 g L^{-1}) was added to the medium to match the salinity level detected in the water column of the wetland selected as the model of study. Three different concentrations of bulk (unfiltered) PPHS were established: 50, 200, and 500 mg L^{-1}. Basal medium without added PPHS was also prepared for control microcosms. All media were flushed with N_2 for 1 h to remove dissolved O_2 in 1 L tight-sealed bottles. These bottles were then introduced into a glovebox (100% N_2, with a copper bed for oxygen removal) to anoxically dispense 75 mL of each solution in 110 mL serum flasks. After all flasks were sealed with rubber stoppers and aluminum rings, they were taken out of the glovebox, their atmosphere was replaced by a mixture of N_2:CO_2 (90/10%) for 10 min, and $NaHCO_3$ was provided as a buffer from a concentrated anoxic stock to a final concentration of 60 mmol L^{-1} (~7.5 final pH). Afterward, sulfide was provided to corresponding treatments from a concentrated anoxic stock to reach an initial concentration of 2 mmol L^{-1}. Dissolved sulfide concentration after equilibrium with the microcosm's headspace was ~ 1.3 mmol L^{-1}, which agreed with the initial circumneutral pH value. The experimental design was as follows: 50 mg PPHS L^{-1} + sulfide, 200 mg PPHS L^{-1} + sulfide, 500 mg PPHS L^{-1} + sulfide, 500 mg PPHS L^{-1} (without sulfide), and sulfide (2 mmol L^{-1}, without PPHS). All treatments were carried out with six experimental replicates, wrapped in aluminum foil to avoid photoreactions, and incubated at 28 °C without shaking. A detailed description of the complete experimental setup is included in SM (Table S1).

Dissolved sulfide determinations

Samples for dissolved sulfide measurements were taken after thoroughly shaking the microcosms and immediately fixed in acid (2% Zn-acetate). Dissolved sulfide determination was immediately performed following the methodology previously proposed by Cline (1969). Briefly, 200 µL of Zn-acetate fixed samples were reacted with *N*,*N*-dimethyl-p-phenyl-diamine, and $NH_4Fe(SO_4)_2$ under highly acidic conditions. The blue coloration produced after 10 min reaction was measured at 664 nm in a microplate reader (FlashScan 550, Analytic Jena, Germany).

Sulfate and thiosulfate determinations

Supernatant aliquots were taken from the microcosms after thorough shaking and mixed with concentrated Zn-acetate to precipitate the remaining dissolved sulfide and avoid the additional formation of sulfate and/or thiosulfate coming from oxidation by air. After the reaction, samples were centrifuged for 10 min at 10,000 rpm and the supernatant was recovered and preserved at − 20 °C until analysis. Sulfate and thiosulfate analysis was performed using an ion chromatography instrument (Metrohm 883 Basic IC Plus) equipped with a Metrohm 863 compact autosampler, a Metrosepp A supp4 250/4.0 column, and a MetroseppRP2 guard/3.5 precolumn. The eluent used was a mixture of Na_2CO_3 1 mmol L^{-1}, $NaHCO_3$ 4 mmol L^{-1}, and 5% acetone.

Elemental sulfur determinations

Zn-acetate fixed supernatant aliquots were periodically sampled and preserved at − 20 °C until analysis. Thawed samples were filtrated with polytetrafluoroethylene membrane filters (0.22 µm) and derivatized with methanol before analysis. Elemental sulfur was analyzed by HPLC according to the protocol described by Lohmayer et al. (2014).

Incorporation of sulfur into the structure of NOM

The fate of sulfurous compounds by incorporation into NOM was explored by analysis of freeze-dried organic content of the microcosms by Fourier-transform infrared spectroscopy (FTIR). KBr pellets with approximately 1% (v/v) of the freeze-dried PPHS sample (after reaction with dissolved sulfide and PPHS without reaction as control) were made and analyzed in a Bruker VERTEX 80v instrument (Ettlingen, Germany) using KBr pellets without PPHS sample as blank. Data were collected in a range of 4500–370 cm^{-1} at a resolution of 4 cm^{-1} with 100 scans for each sample.

Sediment incubation setup

First incubation cycle

Serum flasks (110 mL) were inoculated with sediments from a coastal wetland in which microbiota were previously detected to perform AOM (Valenzuela et al. 2017). The sediment was collected from the Sisal wetland located in the Yucatán Peninsula (southeastern Mexico) and maintained under anoxic conditions at 4 °C until inoculation. Further details on the sampling site and sediment collection methodology are provided in a previous report (Valenzuela et al. 2020). For inoculation, ~2 g of homogenized wet sediment was dispensed into the serum flasks inside the previously described glovebox. No pretreatments were performed on the sediment before inoculation apart from removing excess water by decantation and removing big solid particles (soil granules and vegetation remains) manually. After sediment inoculation into the bottles, 80 mL of anoxic basal medium (previously bubbled for 1 h with N_2) enriched with 500 mg L^{-1} of PPHS were dispensed into an appropriate number of serum flasks while anoxic basal medium lacking PPHS was dispensed into additional flasks to serve as controls. Experimental treatments including sulfate, in the presence and absence of PPHS, were done by spiking Na_2SO_4 from an anoxic stock to reach a concentration of 2 mmol L^{-1}. All microcosms were tightly sealed with rubber stoppers and aluminum rings before taking them out of the glovebox. The stoppers used to seal the microcosms were boiled three times (10 min per boiling cycle), let cool, and finally rinsed with Mili-Q® water before use to avoid microbial inhibition due to potentially toxic chemicals released during incubation (Niemann et al. 2015). Once outside the glovebox, the microcosms' headspace was replaced with a mixture of N_2:CO_2 (90/10%) for 10 min and then $NaHCO_3$ was provided as a buffer from an anoxic concentrated stock to a final concentration of 60 mmol L^{-1} (final pH = ~7.2). Methanotrophy experiments were established by spiking an appropriate number of PPHS-enriched and PPHS-free microcosms with 20 mL of CH_4 (purity > 99%). The same number and type of microcosms were left with N_2:CO_2 atmosphere to serve as methanogenesis controls. Sterile controls including PPHS were made by autoclaving three times. After autoclaving, the same volume of CH_4 as in the main experimental treatment was injected into the flasks' headspace. The microcosms were then incubated in the dark at 28 °C and left stabilizing for 24 h before performing time zero measurements to reach gas-phase stabilization and equilibrium with the liquid medium. A detailed description of the complete experimental setup is included in Supplementary Information (Table S2).

Second incubation cycle

Given that microbial activity plateaued by the end of the first incubation cycle, a second cycle was implemented. This cycle had as purposes (i) to replenish the microcosms with fresh electron acceptors, (ii) to get rid of any inhibitory intermediaries accumulated in the liquid media potentially hindering microbial activities, and (iii) to restore the CH_4 partial pressure and thus avoiding the thermodynamical restriction of the AOM reactions caused by a low availability of dissolved CH_4. To this end, after 20 days of incubation (1st cycle), the flasks' headspace was flushed with N_2. The flasks were then introduced into the glovebox, let settle, and then opened. Afterward, the totality of the liquid content (~80 mL of supernatant) was replaced by a fresh anoxic medium enriched with 1000 mg L^{-1} of PPHS. PPHS were excluded again from the corresponding controls and sulfate was provided from a concentrated anoxic stock to reach a final concentration of 2 mmol L^{-1}. Once outside the glovebox, the microcosms' anoxic conditions were ensured by flushing the headspace with N_2:CO_2 (90/10%) for 10 min, and then $NaHCO_3$ was provided as buffer to a final concentration of 60 mmol L^{-1}. The second incubation cycle started after spiking 20 mL of CH_4 into the microcosms' headspace in the case of the methanotrophy set of microcosms. On day 10 of the second incubation cycle, sulfate was spiked into the corresponding microcosms from an anoxic concentrated stock to provide a surplus concentration of 2 mmol L^{-1} to stimulate sulfate-reducing activities.

Methane measurements

Changes in methane concentrations in the microcosms' headspace were determined by injecting 100 µL of the headspace gas into a gas chromatograph SRI 8610C (SRI Instruments, Europe GMBH, Germany) equipped with a packed column (0.3-m HaySep-D

packed Teflon; Restek, Bellefonte, USA) at 42 °C, and a thermal conductivity detector at 111 °C (detection limit 2 ppmv). N_2 was used as the carrier gas at a flow rate of 20 mL min^{-1}.

Methanotrophic and methanogenic rates calculation

AOM activities were evaluated by means of the linear regression of the maximum slope of decreasing methane concentrations considering at least three consecutive sampling points. Methanogenic rates were calculated by linear regressions of the maximum slope with at least three consecutive sampling points in which methane concentrations increased in time.

Results

Inorganic products derived from sulfide oxidation driven by the electron-accepting capacity of PPHS

All experimental treatments containing PPHS showed sulfide transformation driven by the oxidizing power of PPHS during 8 h of chemical reaction (Fig. S1). The maximum rates of sulfide oxidation correlated with those of formation products (S^0, $S_2O_3^{2-}$) and showed dependency on the increasing concentrations of PPHS (Fig. 1).

The preferential product during abiotic sulfide oxidation under all the PPHS concentrations tested was elemental sulfur. This outcome is in line with thermodynamic predictions (Eq. 2). For instance, sulfide oxidation to elemental sulfur is possible for a NOM's standard redox potential range from −260 to +300 mV, while the oxidation of sulfide to thiosulfate is only possible in a narrower range going from +20 to +300 mV (Fig. 2). Furthermore, this outcome is in line with a previous study evaluating sulfide oxidation by dissolved organic matter (DOM) (Yu et al. 2015). The highest rate of elemental sulfur formation recorded was 20.2 ± 0.6 µmol L^{-1} h^{-1} at a PPHS concentration of 500 mg L^{-1} (Fig. 1A). Mass balances performed using those values obtained at the end of the experiment revealed that from the total amount of oxidized sulfide 48, 67, and 76% of the S was transformed into S^0 at PPHS concentrations of 50, 200, and 500 mg L^{-1}, respectively (Fig. 1B).

In addition to being less thermodynamically favorable than elemental sulfur formation (Fig. 2), the thiosulfate production reaction was also slower than the former under all the conditions tested (Fig. 1). The highest thiosulfate production rate of 2.83 ± 0.65 µmol L^{-1} h^{-1}, obtained with the PPHS concentration of 500 mg L^{-1}, was ~ 50-fold lower than the highest rate of S^0 production under the same conditions (Fig. 1A). Contrary to what we observed for elemental sulfur in which the percentage of sulfide oxidized was directly affected by the increasing PPHS concentrations, the percentage of sulfide oxidized to thiosulfate remained almost constant with increasing PPHS concentrations at values ranging from ~ 17 to 20% (Fig. 1B). Concerning sulfate, the most oxidized form of S, low levels of this product, which

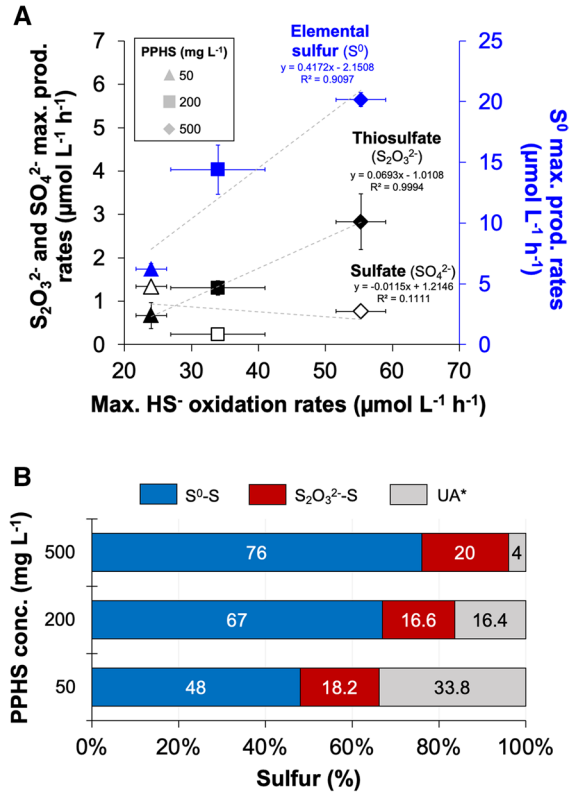

Fig. 1 Analysis of products originating from dissolved sulfide (HS^-) abiotic oxidation with Pahokee Peat humic substances (PPHS) as the terminal electron acceptor. Panel **A** shows the relation between the rates of dissolved sulfide (HS^-) consumption and the rates of zero-valent sulfur (S^0), thiosulfate ($S_2O_3^{2-}$) and sulfate (SO_4^{2-}) production. Panel **B** displays a sulfur mass balance considering the amounts of HS^- oxidized, and those of S^0 and $S_2O_3^{2-}$ (produced). All data represent the mean and standard error of experimental triplicates. *UA: unaccounted

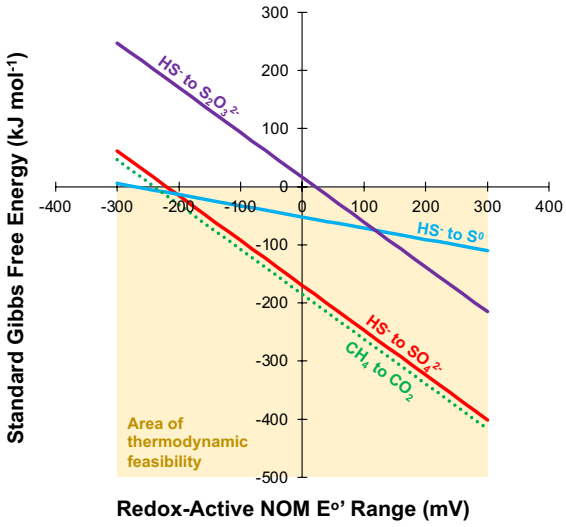

Fig. 2 Graphic representation of the range of thermodynamic feasibility of sulfide and methane oxidation reactions with redox-active NOM as terminal electron acceptor. The reactions displayed are: sulfide (HS^-) oxidation to elemental sulfur S^0 (blue), sulfide oxidation to thiosulfate ($S_2O_3^{2-}$) (purple), sulfide oxidation to sulfate (SO_4^{2-}) (red), and methane (CH_4) anaerobic oxidation to carbon dioxide (CO_2) (green). Chemical (abiotic) and microbially mediated reactions are depicted with continuous and dotted lines, respectively. Displayed thermodynamic calculations were performed under standard conditions (pH = 7, T = 25 °C) and considering a range of standard redox potential value ($E^{o'}$) from −300 to +300 mV for redox-active NOM

did not correlate with the PPHS concentrations, were detected under all experimental conditions, including controls lacking PPHS (Figs. 1A and S1). In previous similar studies, the possibility of sulfate being generated due to reaction with traces of oxygen during sampling and sample analysis has been considered (Heitmann and Blodau 2006).

Formation of S-bearing moieties in PPHS

The formation of several sulfur-containing chemical moieties derived from the reaction of sulfide with PPHS was confirmed by FTIR analysis (Socrates 2004). The formation of functional groups, identified as methylthio, ethylthio, thiol, and aromatic-disulfide/polysulfide was confirmed from these reactions, but they were not detected in controls lacking sulfide (Fig. 3). These findings match with previous studies in which S was incorporated into several sources of NOM and model compounds, such as free quinones (juglone) (Perlinger et al. 2002), DOM from an ombrotrophic bog (Heitmann and Blodau 2006), and Sigma Aldrich humic acids (Yu et al. 2015).

According to these observations, the percentage of S missing in the mass balance might be at least partially explained by sulfur that was incorporated into S-bearing moieties in the organic structure of PPHS (Fig. 1B). While some studies have registered the

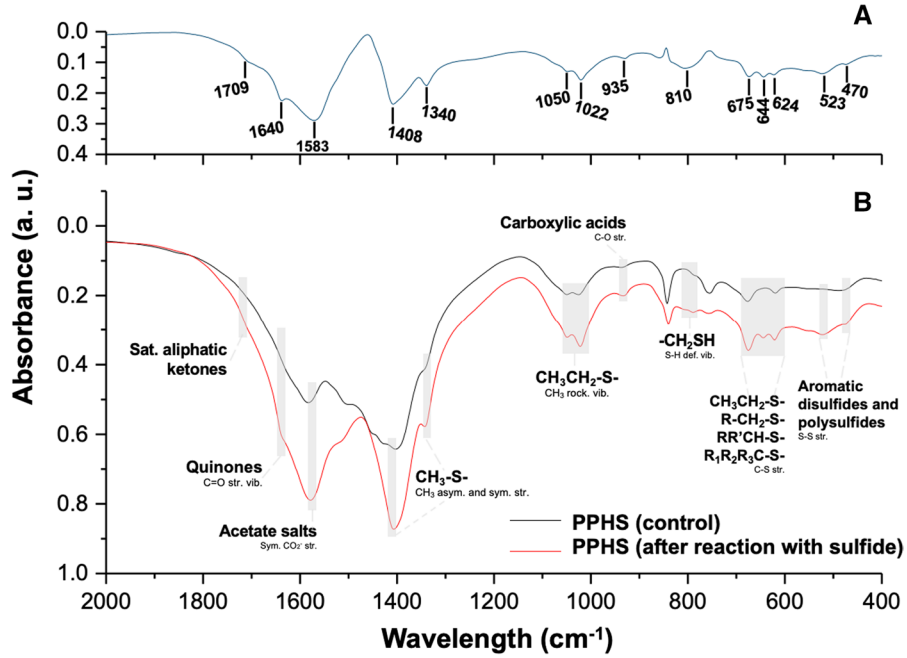

Fig. 3 Fourier-transformed infrared (FTIR) spectra of Pahokee Peat humic substances (PPHS) after abiotic reaction with dissolved sulfide. Panel **A** displays the changes in intensity of peaks determined by using PPHS controls (without reaction with sulfide) as reference to correct the base line. Those signals whose intensity increased after reaction with sulfide are labelled in panel **B**, with spectra obtained for both treatments shown. *Abbreviations corresponding to each of the chemical bond vibrations detected: *vib.* vibrations, *sym.* symmetric, *asym.* asymmetric, *rock.* rocking, *str.* stretching, *def.* deformation

incorporation of up to ~ 60% of the S involved in the reaction into organic compounds (Heitmann and Blodau 2006), we cannot discard the formation of additional inorganic S species such as sulfite and multiple types of polysulfides which were not detected by the analytical techniques employed here, but have been reported elsewhere as a products from similar sulfide oxidation reactions (Jorgensen and Bak 1991; Holmkvist et al. 2011).

Anaerobic methane oxidation

Right after starting the incubation period, CH_4 dynamics were governed by methanogenesis as revealed by raises in the CH_4 concentrations observed during the first 3 to 6 days of incubation depending on the treatment (Fig. 4). This methanogenic activity might have been fueled either by sediment intrinsic organic compounds but also by degradable fractions of the added PPHS as revealed by ^{13}C tracing in a previous report (Valenzuela et al. 2017). After the methanogenic period, AOM activities took place as revealed by decreases in CH_4 concentrations which varied in rate and extent depending on the electron acceptor(s) present in each treatment. The highest maximum AOM rate registered during the first incubation cycle (18.6 ± 2.5 µmol CH_4 L^{-1} day^{-1}) was observed in the experimental treatment with PPHS and sulfate (Fig. 4A). In comparison, the maximum AOM rate in the presence of PPHS as the only TEA (10.7 ± 1.7 µmol CH_4 L^{-1} day^{-1}) was ~ 43% lower than that observed in the presence of both sulfate and PPHS. The lowest AOM activities during this cycle were detected in the treatment containing only sulfate and were statistically comparable to those obtained in the experimental controls lacking any external TEA (~ 6.3 µmol CH_4 L^{-1} day^{-1}) (Fig. 4B).

During the second incubation cycle, in which the concentration of PPHS was doubled with respect to the first cycle, the highest AOM activity was

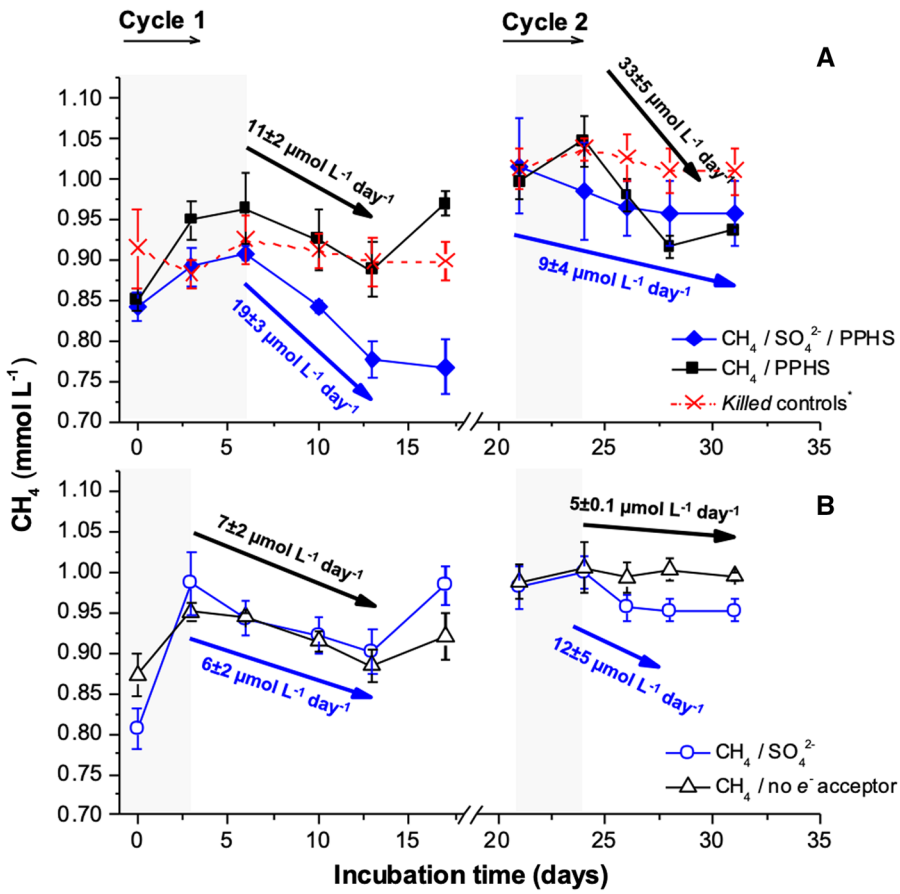

Fig. 4 Methane dynamics in wetland sediment incubations under methanotrophic conditions as affected by sulfate (SO_4^{2-}) and/or Pahokee Peat Humic Substances (PPHS) as terminal electron acceptors. Panel **A** depicts those treatments containing PPHS while Panel **B** depicts controls lacking PPHS. Shaded areas represent the methanogenic phase detected right after each incubation period started. All data represent the mean and standard error values of experimental triplicates. Rates of anaerobic methane oxidation are presented with arrows and were calculated by linear regression considering at least three sampling points of consistent decline in CH_4 concentrations

recorded in the PPHS treatment (32.8 ± 4.9 μmol CH_4 L^{-1} day^{-1}). This rate was twice as high as that observed during the first incubation cycle evidencing the clear effect of doubling the concentration of PPHS on the methanotrophic activity. Contrastingly, AOM maximum rates in those treatments containing both sulfate and PPHS, as well as with sulfate alone, and in the controls without added TEA were ~ 72, ~ 64, and ~ 86% lower with respect to the first cycle, respectively (Fig. 4A). Furthermore, supply of additional sulfate after the first half of the second incubation cycle (incubation day 26) did not stimulate sulfate-dependent AOM activity (Eq. 5).

Methanogenic activity

Confirming what was observed in the AOM setup, significant methanogenic rates were observed during the incubation period in those experiments lacking added CH_4 (Fig. 5). The highest methanogenic rates during the first incubation cycle were obtained in the PPHS amended treatment (52.7 ± 15.1 μmol CH_4 L^{-1} day^{-1}) followed by the controls without added TEA (30.2 ± 6.5 μmol CH_4 L^{-1} day^{-1}) (Fig. 5A). The lowest methanogenic activity during this incubation period was observed in the experimental treatment containing both TEAs (sulfate + PPHS) (7.5 ± 1.9 μmol CH_4 L^{-1} day^{-1}), while slight CH_4 production was only observed during the first 3 days of incubation followed by minor decreases over the rest of the incubation period (Fig. 5A).

During the second incubation cycle, the only detectable methanogenic activity was registered in the controls lacking added TEA (0.04 ± 0.005 μmol CH_4 L^{-1} day^{-1}) (Fig. 5B). This outcome suggests that under the very limited availability of intrinsic electron

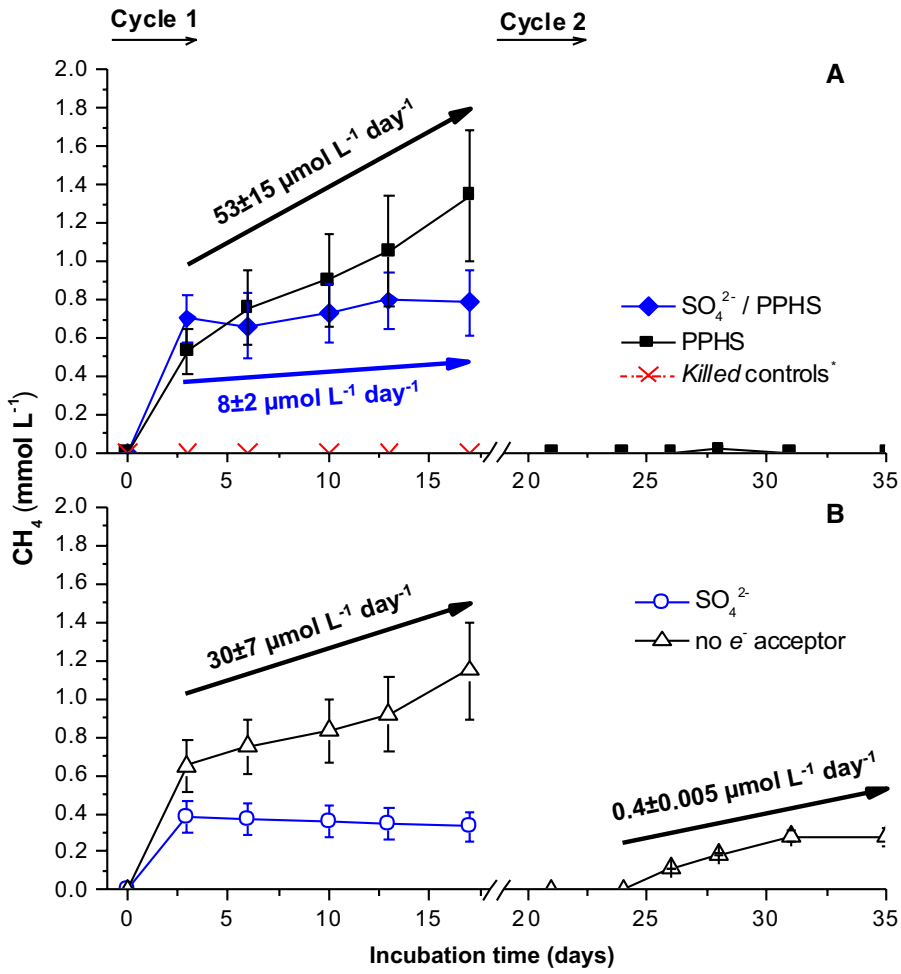

Fig. 5 Methanogenesis performed by wetland sediment microbiota as affected by sulfate (SO_4^{2-}) and Pahokee Peat Humic Substances (PPHS) as terminal electron acceptors. All data represent the mean and standard error values of experimental triplicates. Rates of methanogenesis are presented with arrows and were calculated by linear regression considering at least three sampling points of consistent increase in CH_4 concentrations

donors (labile organic matter), sulfate and PPHS were able to completely suppress CH_4 production fueled by the remaining substrates.

Discussion

The extent to which organic matter degradation produces CO_2 or CH_4 in anoxic ecosystems is importantly affected by redox reactions of sulfide with redox-active moieties in NOM (Blodau and Deppe 2012; Heitmann et al. 2007; Yu et al. 2016a, b). In their oxidized state, these redox-active functional groups can lead to the formation of several organic and inorganic S-compounds which may impact the microbial reactions regulating methane fluxes by means of scarcely explored mechanisms (Fig. 6).

In this study, sulfide oxidation by bulk PPHS, a typical reference of naturally occurring redox-active NOM (Valenzuela et al. 2017; Tian et al. 2018; Xu et al. 2020), resulted in the preferential production of elemental sulfur, with thiosulfate as the second most abundant product (Fig. 1B). While thiosulfate has been previously detected as a key intermediary promoting S-cycling and thus diminishing the amount of carbon available for methanogenesis (Heitmann and Blodau 2006), to the best of our knowledge, there are no systematic studies assessing if elemental sulfur can similarly suppress methanogenesis. Considering that elemental sulfur can be used as TEA by several genera of microorganisms (bacteria and archaea) for the oxidation of a wide range of organic compounds (Hedderich et al. 1998; Zhang et al. 2021), future research should address the role that elemental sulfur, produced via sulfide oxidation with NOM, may play in suppressing CH_4 production in anoxic environments (Fig. 6). Concerning the effect that elemental sulfur may have on AOM, studies have pointed out to this molecule as a key intermediate during sulfate-dependent AOM (Milucka et al. 2012; Hatzikioseyian et al. 2021). Despite this, the direct use of elemental sulfur as TEA for AOM has not been demonstrated, which may be partly due to the thermodynamic restrictions of this reaction (Eq. 7).

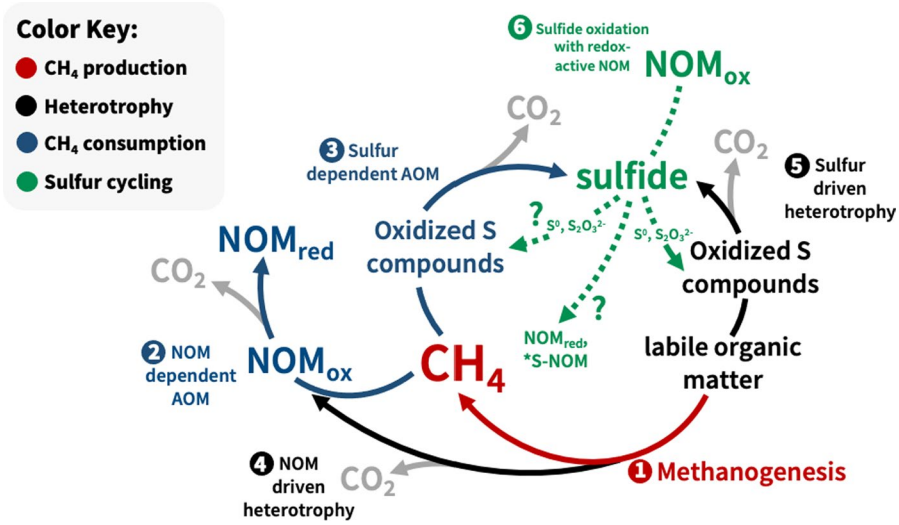

Fig. 6 Schematic representation of C and S cycles including microbial and chemical reactions with a potential impact for CH_4 and CO_2 emissions from anoxic environments. Reaction 1: methanogenesis from labile organic matter. Reactions 2 and 3: anaerobic methane oxidation (AOM) reactions employing oxidized natural organic matter (NOM_{ox}) and oxidized sulfur compounds (i.e., sulfate and thiosulfate) as terminal electron acceptors (TEA). Reactions 4 and 5: heterotrophic reactions employing labile organic matter as electron donor and NOM_{ox} and oxidized sulfur compounds as TEA. Reaction 6: abiotic sulfide oxidation by NOM_{ox} producing partially oxidized inorganic sulfur compounds (thiosulfate and elemental sulfur) as well as NOM containing sulfur-bearing moieties (*S-NOM). Chemical (abiotic) reactions are denoted with dotted lines while microbially catalyzed reactions are denoted with solid lines. Those S cycling reactions triggered by NOM proposed in this work as open questions for future research are denoted by question marks

$$CH_4 + 4S^0 + 3H_2O \rightarrow HCO_3^- + 4HS^- + 5H^+$$
$$\Delta G^{o'}(kJ\,mol^{-1}) = +39 \quad (7)$$

Additional reports on abiotic sulfide oxidation by different sources of NOM have documented that thiosulfate is the sole product of sulfide oxidation (Bauer et al. 2007), or the primary product with elemental sulfur as the secondary S oxidized species (Heitmann and Blodau 2006; Heitmann et al. 2007). Such results divergence from the outcome of the present study (Fig. 1) may be explained by the exceptionally variable features that distinct sources of redox-active NOM and analogues may display (e.g., redox-potential, number, and type of redox-moieties, etc.) (Fig. 2) (Aeschbacher et al. 2010; Yu et al. 2016a, b). Nonetheless, thiosulfate, produced even at low concentrations, might have an important impact on CH_4 cycling processes. Apart from preserving heterotrophic thiosulfate-reducing activities and thus hindering CH_4 production (Fig. 6), the production of thiosulfate from sulfide oxidation by NOM may have unexplored effects in the AOM process, which deserves further investigation. For instance, S-cycling via thiosulfate production could fuel CH_4 consumption by continuously providing thiosulfate to serve as TEA for sustaining AOM (Eq. 6). Such a cryptic cycle has been reported to occur in marine sediments with ferric iron as the sulfide oxidizing agent (Holmkvist et al. 2011). An additional fact supporting the feasibility of this phenomenon is that the microbial consortia catalyzing sulfate-dependent AOM can also use thiosulfate to oxidize CH_4 (Cassarini et al. 2017, 2019).

Based on the evidence gathered throughout the two AOM incubation cycles, NOM-AOM was the main methanotrophic process taking place during the incubations of wetland sediment. This is in line with a previous report based on the same wetland sediment in which sulfate-reducing rates did not account for important AOM activities (Valenzuela et al. 2019). Considering this, sulfate only acted as a methanogenesis suppressor presumably by previously reported mechanisms of competition for organic substrates with methanogens which is in line with previous studies (Figs. 4 and 5) (Lovley and Klug 1983; Gauci et al. 2002, 2004; Pester et al. 2012). These findings imply that even if partially oxidized sulfur products are produced by the electron-accepting capacity in NOM, they may have a null effect on methanotrophy if NOM-reducing biota is responsible for driving AOM instead of sulfate-reducers. Instead of stimulating AOM rates by inducing a cryptic sulfur cycle, sulfate negatively affected AOM when it was present along with PPHS (Fig. 5). This suggests that sulfate-reducing activity may diminish the electron-accepting capacity of redox-active NOM by the chemical reduction of its electron-accepting moieties by the produced sulfide, which could also result in the transformation of these moieties into S-bearing functional groups of unknown chemical reactivity (Figs. 3 and 6) (Zhang et al. 2020; Pham et al. 2022). Apart from NOM-AOM, additional processes importantly diminishing CH_4 production in wetland soils such as NOM-fueled heterotrophy (Keller et al. 2009; Hopple et al. 2019; Rush et al. 2021) might be negatively affected if the electron-accepting capacity of redox-active NOM is depleted by sulfide. These results imply that, in addition to thermodynamic and kinetic constraints, a crucial factor defining the overall effect that S cycling, promoted by redox-active NOM, will have in CH_4 cycling is the composition and metabolic functionalities of the microbial communities involved. For instance, environments, such as deep-sea sediments in which anaerobic methanotrophic archaea (ANME) and sulfate-reducing bacteria catalyze AOM (Orphan et al. 2002; Bhattarai et al. 2019) would be more likely to be subject to stimulation if redox-active NOM contributes to sulfur cycling by providing a suitable TEA (e.g., thiosulfate) (Fig. 6). In the specific case of the sediment employed as a model system for the present study, the typical microbial members catalyzing sulfate-dependent AOM were present at negligible levels in the case of ANME-1 and -3 archaea or completely absent in the case of sulfate-reducing bacteria from the *Desulfosarcina* and *Desulfococcus* genera (Valenzuela et al. 2017).

Finally, future research on the effect of sulfide/NOM reactions in the CH_4 cycle might comprise experimental setups testing the effect of distinct levels of extrinsically provided sulfide on NOM-reducing/CH_4-oxidizing microbial cultures. Furthermore, to improve the evaluation of the rates and extent of NOM-dependent AOM, the utilization of ^{13}C–CH_4 for $^{13}CO_2$ tracing together with the mediated electrochemical analysis of the redox-state of NOM is advised (Li et al. 2020).

Conclusions

The results gathered in this study provide the first pieces of evidence on the impact that sulfide oxidation, provoked by redox-active NOM, might have on novel methanotrophic processes, such as NOM-dependent AOM. Our findings suggest that while elemental sulfur and thiosulfate constitute the main sulfur species coming from sulfide oxidation by NOM, the extent to which these products will affect AOM activities will be negligible if the methanotrophic microbial communities primarily depend on NOM and not on oxidized sulfur compounds (e.g., thiosulfate or sulfate) to perform this reaction. Under this scenario, further studies must focus on deciphering the potential role of sulfide as a competitor of CH_4 as an electron donor for NOM reduction, as well as on elucidating the implications that S incorporation on the structural network of NOM has on its availability as TEA for AOM. Concerning divergent scenarios in which sulfur-dependent AOM is the dominant process, it remains an open question if NOM-catalyzed thiosulfate production will drive a cryptic sulfur cycle fueling AOM. Altogether, the results of this study support previous evidence demonstrating that NOM-driven sulfide oxidation contributes to shaping CH_4-cycling in anoxic environments, still further investigation must be performed considering the pivotal role of CH_4 as one of the most important greenhouse gases driving climate change.

Acknowledgements The authors thank Alejandra Prieto-Davó for wetland sediment sampling, as well as Ellen Roehm, Lars Grimm, Annette Flicker, and Joseph Usack for their technical support. The valuable feedback of the reviewers involved in this manuscript is greatly acknowledged.

Author contributions EIV: conceptualization, investigation, writing—original draft. CB: writing—review & editing, visualization. JF: writing—review and editing, methodology. BP-F: writing—review & editing. AK: resources, writing—review & editing, visualization. FJC: resources, writing—review & editing, visualization.

Funding EIV thanks the German Service for Academic Exchange (DAAD) for grant number 57378443 from the Short-Term Research Grants 2018 program, as well to the National Council of Science and Technology of Mexico (CONACyT) for the PhD fellowship 421676. FJC acknowledges the Grant 682328 provided by CONACYT through the Program Frontiers in Science and DGAPA-UNAM for the research grant PAPIIT-TA200122.

Data availability Enquiries about data availability should be directed to the corresponding author.

Declarations

Conflict of interest The authors declare that they have no known competing financial interests or personal relationships that could have appeared to influence the work reported in this paper.

References

Aeschbacher M, Sander M, Schwarzenbach RP (2010) Novel electrochemical approach to assess the redox properties of humic substances. Environ Sci Technol 44:87–93. https://doi.org/10.1021/es902627p

Aeschbacher M, Vergari D, Schwarzenbach RP, Sander M (2011) Electrochemical analysis of proton and electron transfer equilibria of the reducible moieties in humic acids. Environ Sci Technol 45:8385–8394. https://doi.org/10.1021/es201981g

Bai Y-N, Wang X-N, Wu J et al (2019) Humic substances as electron acceptors for anaerobic oxidation of methane driven by ANME-2d. Water Res 164:114935. https://doi.org/10.1016/j.watres.2019.114935

Bauer M, Heitmann T, Macalady DL, Blodau C (2007) Electron transfer capacities and reaction kinetics of peat dissolved organic matter. Environ Sci Technol 41:139–145. https://doi.org/10.1021/es061323j

Beal EJ, House CH, Orphan VJ (2009) Manganese- and iron-dependent marine methane oxidation. Science 325:184–187. https://doi.org/10.1126/science.1169984

Bhattarai S, Cassarini C, Lens PNL (2019) Physiology and distribution of archaeal methanotrophs that couple anaerobic oxidation of methane with sulfate reduction. Microbiol Mol Biol Rev 83:e00074-e118. https://doi.org/10.1128/MMBR.00074-18

Blodau C, Deppe M (2012) Humic acid addition lowers methane release in peats of the Mer Bleue bog, Canada. Soil Biol Biochem 52:96–98. https://doi.org/10.1016/j.soilbio.2012.04.023

Caldwell S, Laidler J, Brewer EA et al (2008) Anaerobic oxidation of methane- mechanisms, bioenergetics, and the Eecology of associated microorganisms. Environ Sci Technol 42:6791–6799

Cassarini C, Rene ER, Bhattarai S et al (2017) Anaerobic oxidation of methane coupled to thiosulfate reduction in a biotrickling filter. Bioresour Technol 240:214–222. https://doi.org/10.1016/j.biortech.2017.03.003

Cassarini C, Bhattarai S, Rene ER et al (2019) Enrichment of anaerobic methanotrophs in biotrickling filters using different sulfur compounds as electron acceptor. Environ Eng Sci 36:431–443. https://doi.org/10.1089/ees.2018.0283

Cervantes FJ, Velde S, Lettinga G, Field JA (2000) Competition between methanogenesis and quinone respiration for ecologically important substrates in anaerobic consortia. FEMS Microbiol Ecol 34:161–171. https://doi.org/10.1111/j.1574-6941.2000.tb00766.x

Cervantes FJ, De Bok FAM, Duong-Dac T et al (2002) Reduction of humic substances by halorespiring, sulphate-reducing and methanogenic microorganisms. Environ Microbiol 4:51–57. https://doi.org/10.1046/j.1462-2920.2002.00258.x

Cervantes FJ, Gutiérrez CH, López KY et al (2008) Contribution of quinone-reducing microorganisms to the anaerobic biodegradation of organic compounds under different redox conditions. Biodegradation 19:235–246. https://doi.org/10.1007/s10532-007-9130-x

Cline JD (1969) Spectrophotometric determination of hydrogen sulfide in natural waters. Limnol Oceanogr 14:454–458. https://doi.org/10.4319/lo.1969.14.3.0454

Cui M, Ma A, Qi H et al (2015) Anaerobic oxidation of methane: an "active" microbial process. MicrobiologyOpen 4:1–11. https://doi.org/10.1002/mbo3.232

Ettwig KF, Butler MK, Le Paslier D et al (2010) Nitrite-driven anaerobic methane oxidation by oxygenic bacteria. Nature 464:543–548. https://doi.org/10.1038/nature08883

Gauci V, Dise N, Fowler D (2002) Controls on suppression of methane flux from a peat bog subjected to simulated acid rain sulfate deposition. Glob Biogeochem Cycles 16:4-1–4-12. https://doi.org/10.1029/2000gb001370

Gauci V, Matthews E, Dise N et al (2004) Sulfur pollution suppression of the wetland methane source in the 20th and 21st centuries. Proc Natl Acad Sci USA 101:12583–12587. https://doi.org/10.1073/pnas.0404412101

Hatzikioseyian A, Bhattarai S, Cassarini C et al (2021) Dynamic modeling of anaerobic methane oxidation coupled to sulfate reduction: role of elemental sulfur as intermediate. Bioprocess Biosyst Eng 44:855–874. https://doi.org/10.1007/s00449-020-02495-2

Hedderich R, Klimmek O, Kröger A et al (1998) Anaerobic respiration with elemental sulfur and with disulfides. FEMS Microbiol Rev 22:353–381. https://doi.org/10.1016/S0168-6445(98)00035-7

Heitmann T, Blodau C (2006) Oxidation and incorporation of hydrogen sulfide by dissolved organic matter. Chem Geol 235:12–20. https://doi.org/10.1016/j.chemgeo.2006.05.011

Heitmann T, Goldhammer T, Beer J, Blodau C (2007) Electron transfer of dissolved organic matter and its potential significance for anaerobic respiration in a northern bog. Glob Chang Biol 13:1771–1785. https://doi.org/10.1111/j.1365-2486.2007.01382.x

Hernández-Montoya V, Alvarez LH, Montes-Morán MA, Cervantes FJ (2012) Reduction of quinone and non-quinone redox functional groups in different humic acid samples by geobacter sulfurreducens. Geoderma 183–184:25–31. https://doi.org/10.1016/j.geoderma.2012.03.007

Holmkvist L, Ferdelman TG, Jørgensen BB (2011) A cryptic sulfur cycle driven by iron in the methane zone of marine sediment (Aarhus Bay, Denmark). Geochim Cosmochim Acta 75:3581–3599. https://doi.org/10.1016/j.gca.2011.03.033

Hopple AM, Pfeifer-Meister L, Zalman CA et al (2019) Does dissolved organic matter or solid peat fuel anaerobic respiration in peatlands? Geoderma 349:79–87. https://doi.org/10.1016/j.geoderma.2019.04.040

Jorgensen BB, Bak F (1991) Pathways and microbiology of thiosulfate transformations and sulfate reduction in a marine sediment (Kattegat, Denmark). Appl Environ Microbiol 57:847–856. https://doi.org/10.1128/aem.57.3.847-856.1991

Keller JK, Weisenhorn PB, Megonigal JP (2009) Humic acids as electron acceptors in wetland decomposition. Soil Biol Biochem 41:1518–1522. https://doi.org/10.1016/j.soilbio.2009.04.008

Knittel K, Boetius A (2009) Anaerobic oxidation of methane: progress with an unknown process. Annu Rev Microbiol 63:311–334. https://doi.org/10.1146/annurev.micro.61.080706.093130

Leu AO, Cai C, Mcilroy SJ et al (2020) Anaerobic methane oxidation coupled to manganese reduction by members of the methanoperedenaceae. ISME J. https://doi.org/10.1038/s41396-020-0590-x

Li S, Kappler A, Zhu Y, Haderlein SB (2020) Mediated electrochemical analysis as emerging tool to unravel links between microbial redox cycling of natural organic matter and anoxic nitrogen cycling. Earth-Sci Rev 208:103281

Lipczynska-Kochany E (2018) Humic substances, their microbial interactions and effects on biological transformations of organic pollutants in water and soil: a review. Chemosphere 202:420–437. https://doi.org/10.1016/j.chemosphere.2018.03.104

Lohmayer R, Kappler A, Lösekann-Behrens T, Planer-Friedrich B (2014) Sulfur species as redox partners and electron shuttles for ferrihydrite reduction by Sulfurospirillum deleyianum. Appl Environ Microbiol 80:3141–3149. https://doi.org/10.1128/AEM.04220-13

Lovley DR, Klug MJ (1983) Sulfate reducers can outcompete methanogens at freshwater sulfate concentrations. Appl Environ Microbiol 45:187–192. https://doi.org/10.1128/aem.45.1.187-192.1983

Lovley DR, Coates JD, Blunt-Harris EL et al (1996) Humic substances as electron acceptors for microbial respiration. Nature 382:445–448. https://doi.org/10.1038/382445a0

MacCarthy P (2007) The principles of humic substances: An introduction to the first principle. In: Humic substances. Royal Society of Chemistry, Cambridge, pp 19–30

Martinez CM, Alvarez LH, Celis LB, Cervantes FJ (2013) Humus-reducing microorganisms and their valuable contribution in environmental processes. Appl Microbiol Biotechnol 97:10293–10308. https://doi.org/10.1007/s00253-013-5350-7

Milucka J, Ferdelman TG, Polerecky L et al (2012) Zero-valent sulphur is a key intermediate in marine methane oxidation. Nature 491:541–546. https://doi.org/10.1038/nature11656

Niemann H, Steinle L, Blees J et al (2015) Toxic effects of lab-grade butyl rubber stoppers on aerobic methane oxidation. Limnol Oceanogr Methods 13:40–52. https://doi.org/10.1002/lom3.10005

Orphan VJ, House CH, Hinrichs K-U et al (2002) Multiple archaeal groups mediate methane oxidation in anoxic cold seep sediments. Proc Natl Acad Sci 99:7663–7668. https://doi.org/10.1073/pnas.072210299

Perlinger JA, Kalluri VM, Venkatapathy R, Angst W (2002) Addition of hydrogen sulfide to juglone. Environ Sci Technol 36:2663–2669. https://doi.org/10.1021/es015602c

Pester M, Knorr KH, Friedrich MW et al (2012) Sulfate-reducing microorganisms in wetlands—fameless actors in carbon cycling and climate change. Front Microbiol 3:1–19. https://doi.org/10.3389/fmicb.2012.00072

Pham DM, Oji H, Yagi S et al (2022) Sulfur in humin as a redox-active element for extracellular electron transfer. Geoderma 408:115580. https://doi.org/10.1016/j.geoderma.2021.115580

Raghoebarsing A, Pol A, van de Pas-Schoonen K et al (2006) A microbial consortium couples anaerobic methane oxidation to denitrification. Nature 440:918–921. https://doi.org/10.1038/nature04617

Rush JE, Zalman CA, Woerndle G et al (2021) Warming promotes the use of organic matter as an electron acceptor in a peatland. Geoderma 401:115303. https://doi.org/10.1016/j.geoderma.2021.115303

Scheller S, Yu H, Chadwick GL et al (2016) Artificial electron acceptors decouple archaeal methane oxidation from sulfate reduction. Science 351:703–707. https://doi.org/10.1126/science.aad7154

Scott DT, Mcknight DM, Blunt-Harris EL et al (1998) Quinone moieties act as electron acceptors in the reduction of humic substances by humics-reducing microorganisms. Environ Sci Technol 32:2984–2989. https://doi.org/10.1021/es980272q

Shi LD, Guo T, Lv PL et al (2020) Coupled anaerobic methane oxidation and reductive arsenic mobilization in wetland soils. Nat Geosci. https://doi.org/10.1038/s41561-020-00659-z

Socrates G (2004) Infrared and Raman characteristic group frequencies. Wiley, Hoboken

Stevenson FJ (1983) Humus chemistry: genesis, composition, reactions. Nature 303:835–836. https://doi.org/10.1016/0146-6380(83)90043-8

Straub KL, Benz M, Schink B (2000) Iron metabolism in anoxic environments at near neutral pH. FEMS Microbiol Ecol 34:181–186. https://doi.org/10.1016/S0168-6496(00)00088-X

Struyk Z, Sposito G (2001) Redox properties of humic acids. Geoderma 102:329–346

Tian W, Yang Z, Zhang X et al (2018) Redox properties of humic substances under different environmental conditions. Environ Sci Pollut Res 25:25734–25743. https://doi.org/10.1007/s11356-017-9506-3

Valenzuela EI, Cervantes FJ (2021) The role of humic substances in mitigating greenhouse gases emissions: current knowledge and research gaps. Sci Total Environ 750:141677. https://doi.org/10.1016/j.scitotenv.2020.141677

Valenzuela EI, Prieto-Davó A, López-Lozano NE et al (2017) Anaerobic methane oxidation driven by microbial reduction of natural organic matter in a tropical wetland. Appl Environ Microbiol. https://doi.org/10.1128/AEM.00645-17

Valenzuela EI, Avendaño KA, Balagurusamy N et al (2019) Electron shuttling mediated by humic substances fuels anaerobic methane oxidation and carbon burial in wetland sediments. Sci Total Environ 650:2674–2684. https://doi.org/10.1016/j.scitotenv.2018.09.388

Valenzuela EI, Padilla-Loma C, Gómez-Hernández N et al (2020) Humic substances mediate anaerobic methane oxidation linked to nitrous oxide reduction in wetland sediments. Front Microbiol 11:587. https://doi.org/10.3389/fmicb.2020.00587

van Grinsven S, Sinninghe Damsté JS, Villanueva L (2020) Assessing the effect of humic substances and Fe(III) as potential electron acceptors for anaerobic methane oxidation in a marine anoxic system. Microorganisms 8:1288. https://doi.org/10.3390/microorganisms8091288

Vigderovich H, Eckert W, Elul M et al (2022) Long-term incubations provide insight into the mechanisms of anaerobic oxidation of methane in methanogenic lake sediments. Biogeosciences 19:2313–2331. https://doi.org/10.5194/bg-19-2313-2022

Xu Z, Yang Z, Wang H, Jiang J (2020) Assessing redox properties of natural organic matters with regard to electron exchange capacity and redox-active functional groups. J Chem 2020:1–8. https://doi.org/10.1155/2020/2698213

Yu ZG, Peiffer S, Göttlicher J, Knorr KH (2015) Electron transfer budgets and kinetics of abiotic oxidation and incorporation of aqueous sulfide by dissolved organic matter. Environ Sci Technol 49:5441–5449. https://doi.org/10.1021/es505531u

Yu Z, Göttlicher J, Steininger R, Knorr K-H (2016a) Organic sulfur and organic matter redox processes contribute to electron flow in anoxic incubations of peat. Environ Chem 13:816. https://doi.org/10.1071/EN15091

Yu ZG, Orsetti S, Haderlein SB, Knorr KH (2016b) Electron transfer between sulfide and humic acid: electrochemical evaluation of the reactivity of sigma-aldrich humic acid toward sulfide. Aquat Geochem 22:117–130. https://doi.org/10.1007/s10498-015-9280-0

Zhang Y, Zhang Z, Liu W, Chen Y (2020) New applications of quinone redox mediators: modifying nature-derived materials for anaerobic biotransformation process. Sci Total Environ 744:140652. https://doi.org/10.1016/j.scitotenv.2020.140652

Zhang L, Qiu YY, Zhou Y et al (2021) Elemental sulfur as electron donor and/or acceptor: mechanisms, applications and perspectives for biological water and wastewater treatment. Water Res 202:117373. https://doi.org/10.1016/j.watres.2021.117373